Available online at www.sciencedirect.com
SCIENCE DIRECT®
Journal of Solid State Chemistry 177 (2004) 3469–3478
JOURNAL OF SOLID STATE CHEMISTRY
http://elsevier.com/locate/jssc

Non-stoichiometric 1:2 ordered perovskites in the $Ba(Li_{1/4}Nb_{3/4})O_3$–$Ba(Li_{2/5}W_{3/5})O_3$ system

Hui Wu and Peter K. Davies*

Department of Materials Science & Engineering, University of Pennsylvania, 3231 Walnut Street, Philadelphia, PA 19104-6272, USA

Received 1 March 2004; received in revised form 19 May 2004; accepted 20 May 2004

Available online 11 August 2004

Abstract

Although both end members in the $(1-x)Ba(Li_{1/4}Nb_{3/4})O_3$–$xBa(Li_{2/5}W_{3/5})O_3$ (BLNW) system adopt a hexagonal perovskite structure, *B*-site ordered cubic perovskites are formed for the majority of their solid solutions ($0.238 \leqslant x \leqslant 0.833$). Within this range, single-phase 1:2 order ($P\bar{3}m1$, $a \approx \sqrt{2}a_c$, $c \approx \sqrt{3}a_c$) is stabilized for $0.238 \leqslant x \leqslant 0.385$. In contrast to all known $A(B^{I}_{1/3}B^{II}_{2/3})O_3$ perovskites, the 1:2 ordered BLNW solid solutions do not include any composition with a 1:2 cation distribution and the structure exhibits extensive non-stoichiometry. Structure refinements support a model where Li and W occupy different positions and Nb is distributed on both sites, i.e. $Ba[(Li_{3/4+y/2}Nb_{1/4-y/2})_{1/3}(Nb_{1-y}W_y)_{2/3}]O_3$ ($y = 0.21-0.35$, where $y = 0.9x$). The stabilization of the non-stoichiometric order arises from the large charge/size site differences; the loss of 1:2 order for W-rich compositions is related to local charge imbalances on the *A*-site sub-lattice. The range of single-phase 1:1 order is confined to $x = 0.833$, $(Ba(Li_{3/4}Nb_{1/4})_{1/2}(W)_{1/2})O_3$, where the site charge/size difference is maximized and the on-site mismatches are minimized. The microwave dielectric loss properties of the ordered BLNW solid solutions are significantly inferior as compared to their stoichiometric counterparts.

Keywords: Perovskites; Cation order; Non-stoichiometry; Tungstates; Niobates; Rietveld refinement

1. Introduction

Complex barium-based perovskites with the general formula $Ba(B^{I}_{1/3}B^{II}_{2/3})O_3$ (e.g. $Ba(Zn_{1/3}Ta_{2/3})O_3$), which contain a 1:2 ordered arrangement of divalent and pentavalent ions on the octahedral sites, are of commercial importance as low-loss temperature-stable dielectric resonators [1]. The key material properties for these microwave dielectrics include a high relative permittivity ($\varepsilon = 25 \sim 40$), low dielectric loss ($\tan\delta$) or high $Q \times f$ value ($Q \times f = 100-300$ THz, $Q = 1/\tan\delta =$ qualityfactor, $f =$ resonance frequency), and a near-zero temperature coefficient of the resonant frequency (τ_f). Extensive efforts have been made to improve the dielectric properties [2] and understand the dominant mechanism of the dielectric loss in these materials. The type and degree of cation ordering are known to strongly affect the dielectric properties of mixed-metal oxide perovskites [2,3] and the lowest microwave losses are found in systems with a 1:2 ordered structure. In this paper, we describe the first example of a non-stoichiometric 1:2 ordered perovskite discovered in the $(1-x)BaLi_{1/4}Nb_{3/4}O_3$–$xBaLi_{2/5}W_{3/5}O_3$ system.

Although they exhibit outstanding microwave properties, there are relatively few perovskites with a 1:2 *B*-site ordered structure. Most of these compounds belong to the $Ba(B^{2+}_{1/3}B^{5+}_{2/3})O_3$ family, where B^{2+} = Mn, Fe, Co, Ni, Cu, Zn, Mg, Ca, Sr, B^{5+} = Nb, Ta. This list has been supplemented by the recent discovery of two new families with 1:2 ordering of B^{1+}/B^{4+} ($La(Li_{1/3}Ti_{2/3})O_3$) and B^{1+}/B^{5+} (e.g. $(Sr_{2/3}La_{1/3})(Li_{1/3}Nb_{2/3})O_3$, $(Sr_{2/3}La_{1/3})(Li_{1/3}Ta_{2/3})O_3$) [4,5]. In all the known examples, the order is rigidly stoichiometric and the substitution of only 3–5 mol% of a foreign ion with a different size/charge is sufficient to completely destabilize the structure in favor of a 1:1 "random site" arrangement or complete *B*-site disorder (e.g. 3–5 mol% $BaZrO_3$, $BaTiO_3$, $BaCeO_3$, or $La(Zn/Mg)_{2/3}(Nb/Ta)_{1/3})O_3$ in BZN/BMN or BZT/BMT, or 0.5 mol% $Ba(Zn_{1/2}W_{1/2})O_3$) in BZN) [2,6–9].

*Corresponding author. Fax: +215-573-2128.
E-mail address: davies@lrsm.upenn.edu (P.K. Davies).

0022-4596/$ - see front matter © 2004 Elsevier Inc. All rights reserved.
doi:10.1016/j.jssc.2004.05.038

The possible formation of 1:2 ordered phases in the $(1-x)Ba(Li_{1/4}Nb_{3/4})O_3-xBa(Li_{2/5}W_{3/5})O_3$ solid solution system was noted several years ago by Negas et al. [10]. Above 1000°C, $Ba(Li_{1/4}Nb_{3/4})O_3$ forms an eight-layer hexagonal perovskite with an $(hccc)_2$ repeat in a cell with $a = 5.803$ Å, $c = 19.076$ Å. The $Ba(Li_{2/5}W_{3/5})O_3$ or $Ba_{10}Li_4W_6O_{30}$ end-member also adopts a hexagonal structure ($a = 5.760$ Å, $c = 23.742$ Å) in this case, with a 10-layer $(hcccc)_2$ repeat sequence. In the middle of the system, evidence was found for the formation of perovskites with a pure cubic layer repeat. For some compositions, the presence of additional reflections in the X-ray patterns suggested that the cubic phases exhibited ordering of the Li, Nb, W cations on the *B* sites [10], either with a 1:1 "double perovskite structure" or a 1:2 ordered arrangement. However, a complete investigation of the type of order and its range of stability was not conducted.

The present study was carried out to determine the range and identify the type of cation order in the cubic perovskites in the $(1-x)Ba(Li_{1/4}Nb_{3/4})O_3-(x)Ba(Li_{2/5}W_{3/5})O_3$ system. The phase stability and structures were characterized by X-ray and electron diffraction, and Raman spectroscopy; the structures of certain compositions were refined by the Rietveld method using data collected by neutron diffraction, and their microwave dielectric properties were characterized by cavity techniques. The system was found to comprise the first example of a 1:2 ordered perovskite with extensive non-stoichiometry.

2. Experimental

Samples in the $(1-x)Ba(Li_{1/4}Nb_{3/4})O_3-(x)Ba(Li_{2/5}W_{3/5})O_3$ system were prepared with $x = 0.111$, 0.238, 0.333, 0.385, 0.444, 0.556, and 0.833, by conventional solid-state methods. Stoichiometric quantities of the precursors, $BaCO_3$ (Cerac, 99.9%), Nb_2O_5 (Cerac, 99.95%), Li_2CO_3 (Alfa Aeser, 99.0%) and WO_3 (K&K Laboratories, 99.5%), were mixed and calcined in air at 700°C for 10 h in alumina crucibles. The powders were ball milled in polyethylene bottles for 6 h using Y_2O_3 stabilized ZrO_2 balls and ethanol as milling media. The slurry was dried, isostatically pressed into pellets at 80,000 psi and sintered in Pt bags filled with a sacrificial powder of the same composition to prevent any possible loss of lithium, which was monitored by measuring the mass of the samples before and after reaction. Ordered phases could be equilibrated by annealing above 1300°C, and the pellets could be sintered to high density at 1470°C.

Phase identification was conducted with a Rigaku diffractometer using a Cu$K\alpha$ source operated at 45 kV and 30 mA. The unit cell parameters were refined by a least-squares procedure using data collected at slow scan speed ($0.2°\,min^{-1}$) and a step size of 0.02°. Peak positions for the lattice parameter refinements were determined by a Lorentzian fit. For Rietveld refinement, a Scintag PAD X diffractometer was used to measure the powder patterns for values of 2θ from 5° to 120° in 0.02° steps, with a counting time of 12 s for each step. Data processing was carried out using the GSAS package. TEM analysis was performed with a Philips 420 EM operating at 120 kV. Samples for transmission electron microscopy were prepared by disaggregating the ceramics followed by grinding under acetone in an agate mortar. The powder was then suspended in acetone and dispersed onto a lacey carbon 400 mesh TEM grid. Raman data were collected on the sintered pellet surfaces with a Renishaw micro-Raman spectrometer (1 μm beam spot) using a 514.4 nm (2.41 eV) laser line.

Neutron powder diffraction data were collected under ambient conditions using the BT-1 32 detector neutron powder diffractometer at the NIST Center for Neutron Research. A Cu(311) monochromater with a 90° takeoff angle, $\lambda = 1.5404(2)$ Å, and an in-pile collimation of 15 min of arc were used. The sample for neutron powder diffraction was loaded in a vanadium cylinder container. Data were collected over the range of 3–165° 2θ, with a step size of 0.05°. The Rietveld structural refinement was conducted using the GSAS package [11].

The relative permittivity of the samples, ε_r, was measured from 100 Hz to 1 MHz by the parallel-plate method using an HP 4284A precision LCR meter and a Delta 9920 environment chamber from −150°C to 200°C. Measurements of the dielectric loss, $Q = 1/\tan\delta$, and the temperature coefficient of resonant frequency, τ_f, at microwave frequencies were made using cavity methods. To separate the $TE_{01\delta}$ resonance mode from the higher resonance modes, the samples had an aspect ratio (thickness and diameter of samples) close to 0.45. The unloaded Q factor was calculated according to

$$Q = \frac{Q_L}{1 - 10^{-P/20}}, \tag{1}$$

where Q_L is the loaded quality factor determined from the full width of the resonance peak at the 3 dB level and P is the depth of the resonance peak in decibels. The τ_f values refer to the 25–75°C range according to

$$\tau_f = \frac{\Delta f_0}{f_0\,\Delta T}, \tag{2}$$

where Δf_0 is the shift of the resonant frequency, f_0 is the reference frequency at 25°C.

3. Results

The samples of $(1-x)Ba(Li_{1/4}Nb_{3/4})O_3-(x)Ba(Li_{2/5}W_{3/5})O_3$ typically reached equilibrium, as

gauged by the absence of any changes in the X-ray patterns with additional annealing, after heating at 1300–1350°C for 5–10 h. While samples with $x = 0.111$ were comprised of a mixture of cubic and hexagonal phases, single-phase cubic perovskites were formed between $0.238 \leqslant x \leqslant 0.833$ (see Fig. 1). Within this range, the X-ray patterns of compositions with $0.238 \leqslant x \leqslant 0.385$ contained additional reflections at values of 2θ, consistent with the formation of a structure with a 1:2 ordered arrangement of the *B*-site cations. These samples could all be indexed in terms of a 1:2 ordered supercell ($P\bar{3}m1$) with $a \approx \sqrt{2}a_c$, $c \approx \sqrt{3}a_c$; the refined cell parameters are shown in Table 1. For $x = 0.444$ and $x = 0.556$, a second set of ordering reflections associated with 1:1 *B*-site order were also visible and their patterns could be indexed as a two-phase mixture of 1:2 and 1:1 ordered cubic perovskites, with the volume fraction of the 1:1 phase being higher for $x = 0.556$. At $x = 0.833$, $Ba(Nb_{1/8}Li_{3/8}W_{1/2})O_3$, the system forms a single-phase 1:1 ordered, "double" perovskite ($Fm\bar{3}m$) structure with $a = 2a_c = 8.185$ Å, in agreement with the previous results of Negas et al. [10].

The stabilization of 1:2 *B*-site order in this system was confirmed by electron diffraction, which revealed strong superlattice reflections at $k = 1/3[111]_c^*$. The specimens were prepared by cooling the samples in the single-phase 1:2 region from their annealing temperatures at a relatively slow rate (15°C/h) to maximize the size of the ordered domains. An electron diffraction pattern collected from $x = 0.385$ along the $[110]_c$ direction of the pseudocubic sub-cell is shown in Fig. 2(a). The superlattice reflections at $k = 1/3[111]_c^*$ were observed along both of the allowed $\langle 111 \rangle$ directions, due to the existence of a twinned ordered domain structure in this particular diffracting volume [6]. Superlattice reflections at ($h \pm 1/3$, $k \pm 1/3$, $l \pm 1/3$) could also be observed in the [111] direction, Fig. 2(b); the reflections in this and other directions (e.g. $[100]_c$, Fig. 2(c)) were all consistent with those expected for a 1:2 ordered $P\bar{3}m1$ structure. Identical patterns were observed for the other samples in the single-phase 1:2 region.

Table 1
Lattice parameters of 1:2 ordered $(1-x)Ba(Li_{1/4}Nb_{3/4})O_3$–$xBa(Li_{2/5}W_{3/5})O_3$

X	a (Å)	c (Å)	V (Å^3)	c/a
$X = 0.238$	5.796(2)	7.102(1)	206.6(1)	1.2253
$X = 0.333$	5.784(2)	7.108(3)	205.9(1)	1.2286
$X = 0.385$	5.780(3)	7.062(7)	204.3(2)	1.2218

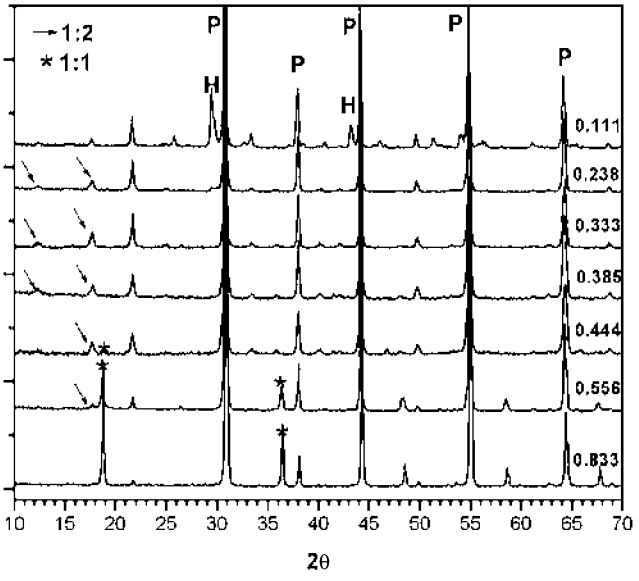

Fig. 1. Powder X-ray patterns of $(1-x)BaLi_{1/4}Nb_{3/4}O_3-(x)BaLi_{2/5}W_{3/5}O_3$ with $x = 0.111$, 0.238, 0.333, 0.385, 0.444, 0.556, 0.833. Main reflections from hexagonal perovskite indicated by H; strongest superlattice associated with the cation order indicated by arrows (1:2 order) and stars (1:1 order).

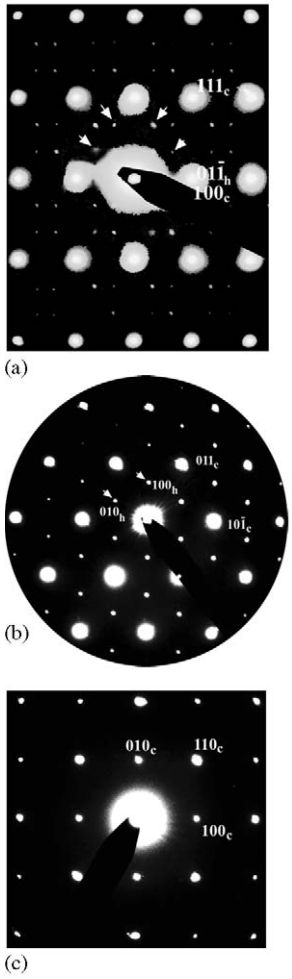

Fig. 2. Selected area electron diffraction patterns collected from 1:2 ordered $x = 0.385$ along: (a) $[110]_c$; (b) $[111]_c$; (c) $[001]_c$. The reflections are indexed in terms of cubic sub-cell (c) and $P\bar{3}m1$ hexagonal supercell (*h*). Superlattice from $1/3[111]_c^*$ ordering are arrowed.

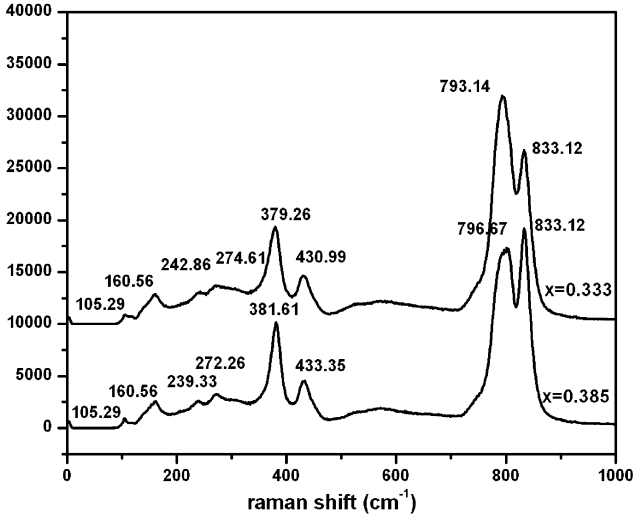

Fig. 3. Raman spectra of the sintered specimens for $x = 0.333$ and $x = 0.385$.

The ordered structures were also probed using Raman spectroscopy, which has been shown to be effective in characterizing the degree and type of cation order in perovskite oxide systems [12,13]. The 1:2 ordered structure has nine Raman-active modes ($4A_{1g} + 5E_g$); however, this can be increased by site disorder of the *B*-site cations [14]. Fig. 3 shows the Raman spectra of the 1:2 ordered $x = 0.333$ and $x = 0.385$ samples. The vibrational spectra are in approximate agreement with the spectra of BMN and BMT, which have the same symmetry [14,15]. The band intensities and frequencies varied with composition, indicating that the Raman spectra are sensitive to the variation of the cation ratios on each *B* site. In the v_1 region, two bands, one at 793 (796) cm^{-1} and the other at about 833 cm^{-1}, were observed and this splitting further confirms the different bonding environments of the two *B*-cation positions in the 1:2 ordered structure.

The stabilization of 1:2 *B*-site order in the $(1-x)Ba(Li_{1/4}Nb_{3/4})O_3$–$(x)Ba(Li_{2/5}W_{3/5})O_3$ system is very unusual. In all the other known examples of the $A(B^{I}_{1/3}B^{II}_{2/3})O_3$ structure, the order is stoichiometric, each site contains a single type of cation and the chemical composition has a 1:2 B^{I}:B^{II} stoichiometry. For the BLNW solid solution system, there is no value of x where a 1:2 ratio of cations can be realized; furthermore, the composition that could be argued to have the highest potential for 1:2 order formation—$Ba(Li_{1/3}Nb_{1/3}W_{1/3})O_3$ ($x = 0.556$) with Li on one position and Nb, W mixed on the other—lies in a two-phase (1:1 + 1:2) region.

For the compositions that actually adopt the 1:2 ordering, a variety of models are possible for the site distributions. To maximize the driving force for order by achieving the largest size and charge difference, the most likely model is one where the lithium and tungsten ions are assumed to occupy different cation sites with niobium distributed on both positions. For this cation distribution, the stoichiometry of the 1:2 ordered phases can be represented as $Ba[(Li_{3/4+y/2}Nb_{1/4-y/2})_{1/3}(Nb_{1-y}W_y)_{2/3}]O_3$, where $y = 0.21-0.35$ and $y = 0.9x$. To examine the validity of this model, refinements of the structure were conducted on a sample with $x = 0.333$ using neutron powder diffraction data.

The Rietveld refinements were performed within the space group $P\bar{3}m1$ (164). The initial atomic positions corresponded to those for an ideal 1:2 ordered arrangement where $a = a_{cubic}\sqrt{2}$ and $c = a_{cubic}\sqrt{3}$. The initial atomic occupancies were based on the model proposed above ($x = 0.333$, $y = 0.3$, has the stoichiometry $Ba[(Li_{0.9}Nb_{0.1})_{1/3}(Nb_{0.7}W_{0.3})_{2/3}]O_3$) with soft constraints imposed on the total Li:Nb:W stoichiometry. The experimental, fitted and difference profiles of the neutron diffraction patterns for the final refined structure are shown in Fig. 4; the refined occupancies and atom positions also yielded a very good fit for the X-ray diffraction powder patterns of the sample (Fig. 5). The final refinement parameters, atomic positions, and selected bond distances and bond valence sums [16] are summarized in Tables 2–4. In agreement with the model, the experimental data for the 1:2 ordered BLNW solid solution provided very clear evidence for the preferential occupation of the B^{II} (2*d*) site by a mixture of Nb and W (~93%), and the B^{I} (1*b*) position by the majority of the Li cations (84%) and the remaining Nb ions. Compared to the ideal stoichiometry predicted by the model, the experimental occupancies corresponded to 7% anti-site disorder. Given that the actual structures are comprised of twinned nano-domains, this apparent disorder could in part be due to localized disorder at the domain boundaries. To test the validity of the "Nb-distribution model", refinements were also conducted for alternate ordering schemes; for example, one involving the distribution of tungsten on both *B* sites (W-distribution model). However, the W-distribution model increased the reliability factor ($R_{wp} = 0.059$, $R_p = 0.045$ compared to $R_{wp} = 0.051$, $R_p = 0.040$), and also gave an inferior fit to the bond valence calculation as reflected by the global instability factor (GII = 0.274 compared to 0.233 for the Nb-distribution model) [17].

The (Nb/W) cations on the B^{II} site show a well-defined displacement away from the center of their octahedra toward the oxygen anions (O1) shared by the B^{I} (Li/Nb) cations, and the resultant (Nb/W)–O1 bond distances (~1.9 Å) are significantly shorter than those for the B^{II}(Nb/W)–O2–B^{II}(Nb/W) linkages (~2.1 Å) (Fig. 6). This displacement is critical in alleviating the over-bonded character of the anions in B^{II}–O2–B^{II} linkages, and is observed in all the known 1:2 ordered phases [18].

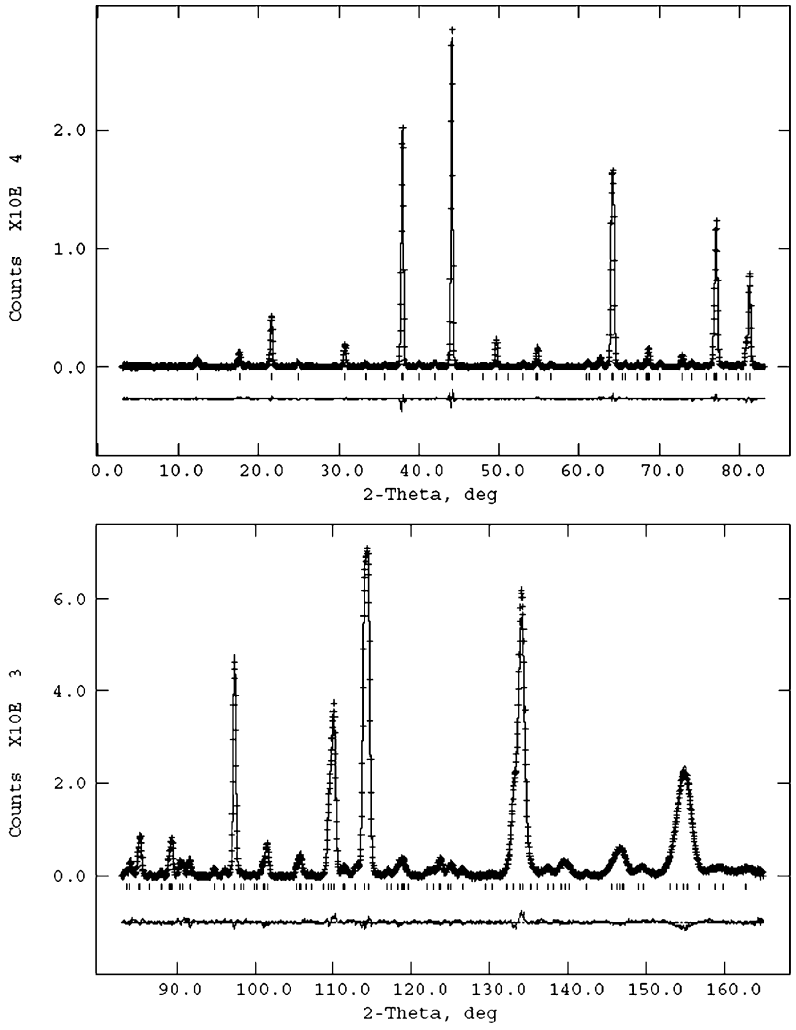

Fig. 4. Experimental (crosses) and calculated (line) and difference neutron diffraction profiles for the 1:2 ordered BLNW with $x = 0.333$.

High-density ($\geqslant$95% theoretical) ceramic samples of BLNW with $x = 0.333$ could be obtained after sintering at 1470°C for 5 h. Measurements of the dielectric properties at microwave frequencies yielded a relative permittivity = 31, a quality factor (Q) = 2432 at 7.813 GHz ($Q \times f = 19,000$), and a temperature coefficient of resonant frequency (τ_f) = +18 ppm/K between 20°C and 80°C.

4. Discussion

Compared to the numerous examples of perovskites exhibiting 1:1 *B*-site cation order, the stabilization of 1:2 order is quite rare. Furthermore, in all the known examples the 1:2 order is stoichiometric, with a single type of cation occupying each site and trace levels of non-stoichiometry inducing a transition to a disordered or double perovskite arrangement. Therefore, the observation of 1:2 order in the $(1-x)Ba(Li_{1/4}Nb_{3/4})O_3$–$(x)Ba(Li_{2/5}W_{3/5})O_3$ (BLNW) system, which does not include any composition with a 1:2 cation stoichiometry, is very unusual. This section begins with an evaluation of the factors responsible for the stabilization and the range of stability of the 1:2 order in this system, followed by a discussion of the possible reasons why these ordered BLNW solid solutions can tolerate such high degrees of non-stoichiometry while the other known isotypes are rigidly stoichiometric.

Although both end-members in the $(1-x)Ba(Li_{1/4}Nb_{3/4})O_3-(x)Ba(Li_{2/5}W_{3/5})O_3$ system adopt a hexagonal perovskite structure involving some degree of face-sharing, a cubic stacking sequence is stable for the majority of their solid solutions ($0.238 \leqslant x \leqslant 0.833$). Within this range, 1:2 order occurs for $0.238 \leqslant x \leqslant 0.385$, 1:1 order is stable for $x = 0.833$, and a two-phase 1:1/1:2 mixture separates the single-phase regions. As the region of stability for 1:2 order does not contain any composition where the different sites in the $Ba(B^{I}_{1/3}B^{II}_{2/3})O_3$ structure could be occupied by a single

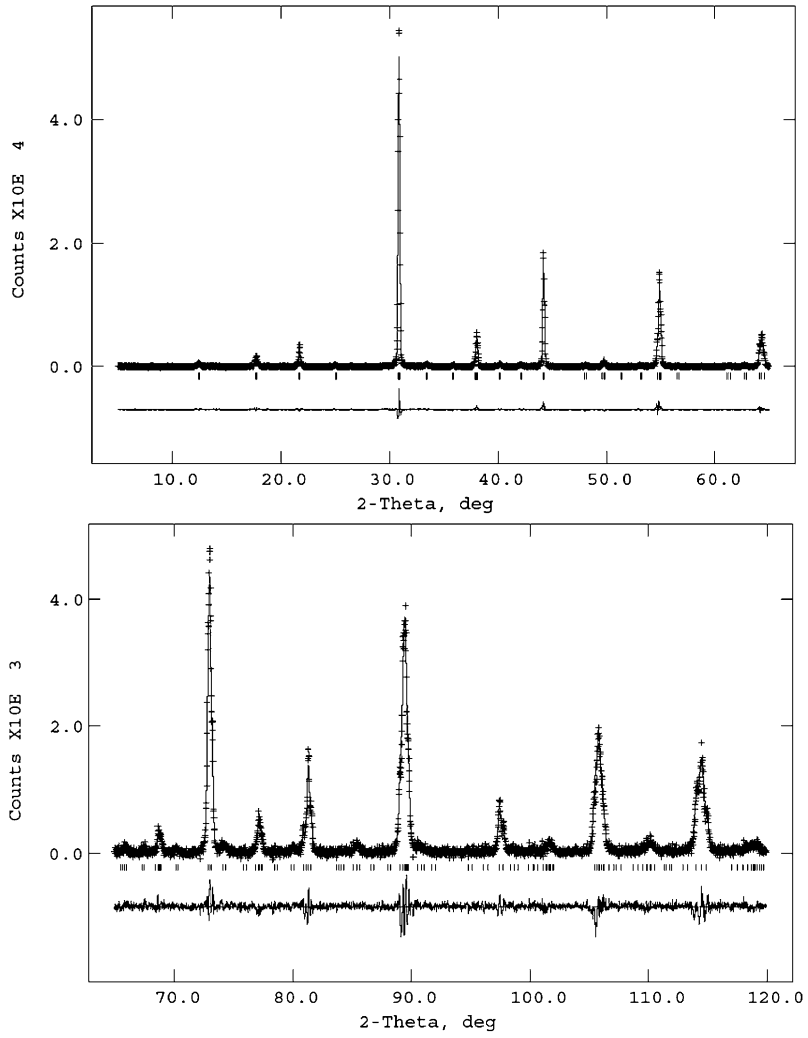

Fig. 5. Experimental (crosses) and calculated (line) and difference X-ray diffraction profiles for the 1:2 ordered BLNW with $x = 0.333$.

Table 2
Crystallographic data from neutron and X-ray diffraction studies for 1:2 ordered $Ba(Nb_{1/2}Li_{3/10}W_{1/5})O_3$, $x = 0.333$

Unit cell (Space group $P\bar{3}m1$, 164)	$a = 5.7910(1)$ Å $c = 7.1267(1)$ Å Volume = 206.980(4) Å^3	
	Neutron	X-ray
R_p (profile)	0.0421	0.0723
R_{wp} (weighted profile)	0.0507	0.0914
R_F^2 (Bragg)	0.0402	0.0586
Reduced χ^2	2.696	1.895
Total refined variables	35	
Minimum 2θ	3	5
Maximum 2θ	165	120
No. of reflections	3239	2748
Profile function	Pseudo–Voight (GSAS type 3)	
Gaussian U, V, W	293, −279, 164	150, −70, 9.6
Cauchy X, Y	0.806, 3.476	1.855, 4.713
Background function	Chebyschev polynomial (14 coefficients)	GSAS type 6 (6 coefficients)

Table 3
Refined structural parameters for 1:2 ordered $Ba(Nb_{1/2}Li_{3/10}W_{1/5})O_3$ using neutron data

Atom	Site	Occupancy	x	y	z	$U \times 100$ Å^2
Ba1	1*a*	1.00	0	0	0	1.02(5)
Ba2	2*d*	1.00	0.3333	0.6666	0.6633 (3)	0.84(3)
Li1	1*b*	0.759(5)	0	0	0.5	1.42(5)
Nb1	1*b*	0.241(5)	0	0	0.5	1.42(5)
Nb2	2*d*	0.630(2)	0.3333	0.6666	0.1748(3)	0.39(2)
W1	2*d*	0.30	0.3333	0.6666	0.1748(3)	0.39(2)
Li2	2*d*	0.070(2)	0.3333	0.6666	0.1748(3)	0.39(2)
O1	6*i*	1.00	0.1729(5)	0.3458(9)	0.3217(2)	1.29(2)
O2	3*e*	1.00	0.5	0	0	1.29(3)

A sites and oxygen sites were assumed to be fully occupied. Lattice parameters $a = 5.7910(1)$ Å, $c = 7.1267(1)$ Å, space group $P\bar{3}m1$ (No. 164).

Table 4
Selected bond distances (Å) and bond valence sums (BVS, v.u.) of constituent atoms in the 1:2 ordered $Ba(Nb_{1/2}Li_{3/10}W_{1/5})O_3$

B site			
Li1/Nb1–O1	$2.149(1) \times 6$	Nb2/W/Li2–O1	$1.919(1) \times 3$
		Nb2/W/Li2–O2	$2.085(1) \times 3$
Average	2.149	Average	2.002
BVS_{obs}	1.48	BVS_{obs}	4.59
BVS_{cal}	1.96	BVS_{cal}	5.02
A site			
Ba1–O1	$2.875(2) \times 6$	Ba2–O1	$2.917(2) \times 3$
Ba1–O2	$2.895(2) \times 6$	Ba2–O1	$2.898(2) \times 6$
		Ba2–O2	$2.924(2) \times 3$
Average	2.885	Average	2.919
BVS_{obs}	2.37	BVS_{obs}	2.22
BVS_{cal}	2.00	BVS_{cal}	2.00

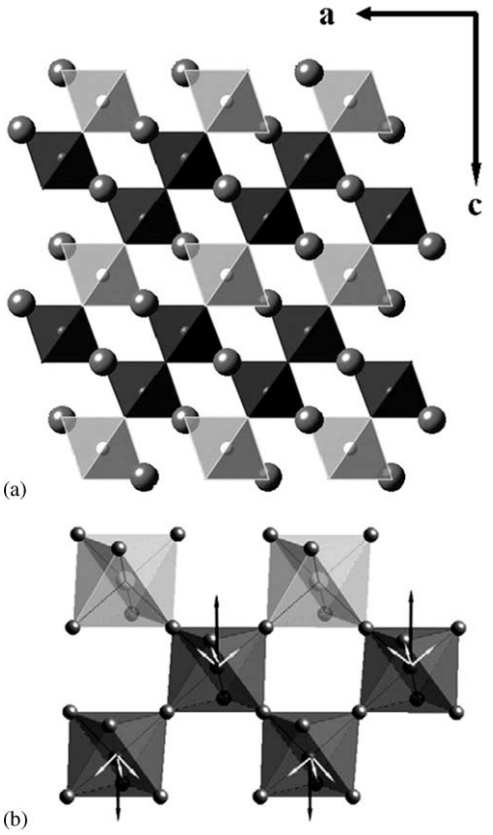

Fig. 6. (a) Refined 1:2 *B*-site ordered $P\bar{3}m1$ structure of BLNW projected along $\langle 110 \rangle_{cub}$ direction; Nb/W octahedra are in dark gray, Li/Nb octahedra are in light gray. The largest spheres represent Ba ions, oxygen is omitted for clarity. Crystallographic directions are given for a cubic sub-cell. (b) Off-centered displacement of B^{II}(Nb/W) cations. O atoms shared at corner are in dark.

type of ion, several models are possible for the arrangement of Li, Nb, and W on the B^I and B^{II} positions. The enthalpic stability of a stoichiometric ordered perovskite increases with the charge and size difference of the two ordered positions. If the ordering involves non-stoichiometry on one or both positions, unfavorable contributions to the enthalpy of ordering will result from the "on-site" size/charge mismatch. The largest B^I/B^{II} size/charge difference and smallest on-site mismatch for a 1:2 ordered structure in the BLNW system occur when Li and W occupy different ordered positions; this arrangement has the general stoichiometry $Ba\{Li_{(3/4+y/2)}Nb_{(1/4-y/2)}\}_{1/3}\{Nb_{(1-y)}W_y\}_{2/3}O_3$, with $0.0 \leqslant y \leqslant 0.5$ and $y = 0.9x$. Direct support for this model was obtained from the structure refinement of the $y = 0.3$ ($x = 0.333$) sample.

The formation of the 1:2 ordered $Ba\{Li_{(3/4+y/2)}Nb_{(1/4-y/2)}\}_{1/3}\{Nb_{(1-y)}W_y\}_{2/3}O_3$ solid solutions is observed over the range $0.21 \leqslant y \leqslant 0.35$; however, the two "end-member" compositions with $y = 0$ ($Ba(Li_{3/4}Nb_{1/4})_{1/3}(Nb)_{2/3}O_3 = Ba(Li_{1/4}Nb_{3/4})O_3$) and $y = 0.5$ ($Ba(Li_{1/3}(Nb_{1/2}W_{1/2})_{2/3}O_3$) lie outside the range of stability and form a hexagonal perovskite and a 1:1/1:2 two-phase mixture, respectively. The stabilization of non-stoichiometric 1:2 order is most likely related to the large difference in the charge (Δq) of the B^I and B^{II} positions, which exceeds +3 when $y > 0$. Order 1:2 first appears for $y = 0.21$ where $\Delta q = 3.61+$ and is maintained up to $y = 0.35$ where $\Delta q = 4.05+$. The site charge difference is significantly higher than that in the well known BZT family of perovskites or the recently discovered $La(Li_{1/3}Ti)_{2/3}O_3$ phase [4] where $\Delta q = 3$, and lies in the same range as the newly reported 1:2 ordered family of $A(Li)_{1/3}(Nb/Ta)_{2/3}O_3$ ($A = Sr_{2/3}La_{1/3}, Ca_{2/3}La_{1/3}$) systems [5]. The increase in Δq with y is accompanied by an increase in the B^I/B^{II} size difference (from 0.09 Å for $y = 0$ to 0.14 Å for $y = 0.5$). The instability of the order for $y \leqslant 0.21$ is presumably associated with the high charge/size mismatch of the Li/Nb ions on the B^I site, which increases as y decreases; however, the absence of 1:2 order in the $0.35 < y \leqslant 0.5$ solid solutions, which should exhibit the highest charge/size site differences and the lowest on-site mismatches, cannot be rationalized using these simple size/charge arguments.

To rationalize the behavior of the W-rich compositions, it is useful to make reference to other W-containing perovskites as well as unpublished studies conducted in our laboratory. Several tungstate cubic perovskites have been reported in the literature, for example $A^{2+}(B^{2+}_{1/2}W_{1/2})O_3$ (A^{2+} = Ba, Sr, Pb, B^{2+} = Ca, Mg, Ni, Zn, etc.) and $A^{2+}(B^{3+}_{2/3}W_{1/3})O_3$ (A^{2+} = Ba, Sr, Pb, B^{3+} = Sc, Fe, Bi); in all cases the *B*-site ions adopt a 1:1 ordered or a disordered arrangement. Few examples are known with both Li and W on the octahedral positions, they include 1:1 ordered $(Sr/Ba)_{1/2}La_{1/2}(Li_{1/2}W_{1/2})O_3$ [19] and $Sr(Li_{2/5}W_{3/5})O_3$ [20] (which in contrast to $Ba(Li_{2/5}W_{3/5})O_3$, is a cubic perovskite). No cubic perovskites have been reported with >60% W on the *B* site. As part of an effort to identify new ordered systems with 1:2 Li:W stoichiometries, we have investigated the feasibility of preparing compounds with the general formulae $A^{5/3+}(Li_{1/3}W_{2/3})O_3$, which have very high size/charge site differences (unpublished work). Several different combinations of *A*-site cations were examined, including $(Sr_{2/3}Na_{1/3})$, $(Sr_{2/3}K_{1/3})$, $(Ba_{2/3}K_{1/3})$, $(Ba_{2/3}Na_{1/3})$, $(Sr_{5/6\square 1/6})$, $(La_{5/9\square 4/9})$, $(La_{1/3}K_{2/3})$, etc.; in all cases, the syntheses yielded multi-phase products that included non-perovskite phases.

It is possible that the instability of these tungstate phases and the loss of 1:2 order in the W-rich BLNW solid solutions are associated with the large imbalance in the local anion bond valences in this structure. If the coordination polyhedra in the 1:2 ordered $A(B^{I}_{1/3}B^{II}_{2/3})O_3$ systems are undistorted, the anions (O2) lying between two B^{II} layers are over-bonded, while those (O1) between a B^{I} and B^{II} layer are under-bonded. Therefore, in all the known 1:2 ordered phases, the B^{II} cations move off the center of their octahedra to lengthen the three B^{II}–O2–B^{II} bonds and shorten the three B^{II}–O1–B^{I} bonds. This type off-centering is typically only observed for small highly charged d^0 cations such as Nb^{5+}, Ta^{5+}, Ti^{4+} (and W^{6+}) that can undergo a second-order Jahn–Teller distortion or cations with a lone pair of electrons (e.g. Bi^{3+}) [21]. The bond valences in a 1:2 ordered form of $A^{1.67+}(Li_{1/3}W_{2/3})O_3$ can be illustrated using the bond graph in Fig. 7. For undistorted coordination polyhedra (Fig. 7(a)), the bond valence requirements of the $A^{1.67+}$, Li^{1+}, and W^{6+} cations (5/36, 1/6, and 1, respectively) lead to a bond valence sum (BVS) = 2.56 for the O2 anions in the B^{II}–O2–B^{II} linkages, and a BVS = 1.72 for the O1 anions in the B^{I}–O1–B^{II} bonds. Because of the higher charge on W, the imbalance is greater than in the BZT-type systems (where BVS O1 = 2.33, O2 = 1.83). If the *A* and B^{I} (Li) polyhedra are assumed to remain ideal, the displacement of W required to produce an ideal BVS at the anion sites can be calculated. For $A^{1.67+}(Li_{1/3}W_{2/3})O_3$, the required bond valence is 23/18 for each W–O1 bond and 13/18 for each W–O2 bond; these correspond to W–O1 and W–O2 bond lengths of 1.826 and 2.039 Å, which can be compared to the ideal (1 valence unit) W–O bond length of 1.917 Å. As the magnitudes of the distortion required for the W–O bonds (where the longer W–O– bond is 6.4% longer than the ideal) are much larger than those required in the BZT-type systems, it is possible that this destabilizes the 1:2 order in the W-rich systems. However, it should be noted that even larger displacements are stable in the ordered hexagonal perovskite $Ba_3W_2O_9$ [22], though here the order involves W^{6+} and vacancies.

We believe a more likely explanation for the loss of 1:2 *B*-site order in W-rich perovskites is related to the incompatibility of the *B*-site distributions with the local charges on the *A*-site lattice. In the 1:2 structure, the $\{\ldots B^{I}B^{II}B^{II}\ldots\}$ layering creates two different environments for the *A*-site cations (see Fig. 8). The A^{I} site is located between two B^{II} layers and has six B^{II} and two B^{I} nearest neighbors; the two A^{II} sites are located

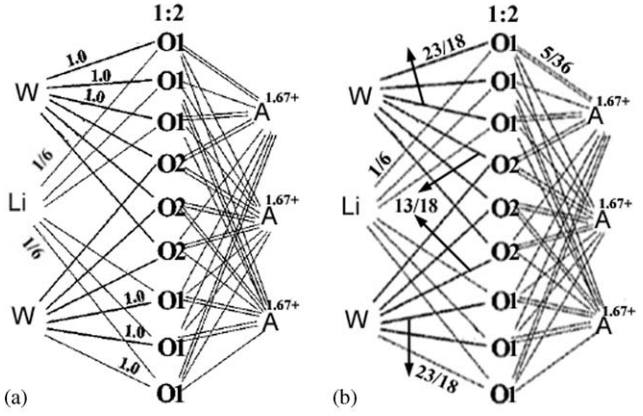

Fig. 7. Bond graph for the hypothetical 1:2 ordered form of $A^{1.67+}(Li_{1/3}W_{2/3})O_3$ without (a) and with (b) octahedral distortion.

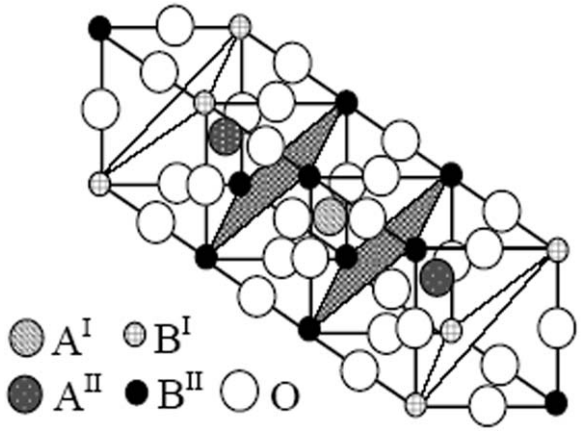

Fig. 8. Different *A*-site environments in the 1:2 $A(B^{I}_{1/3}B^{II}_{2/3})O_3$ structure. A^{I} is located between two B^{II} layers with six B^{II} and two B^{I} nearest neighbors in its sub-cell. A^{II} cation is located between a B^{I} and a B^{II} layer with five B^{II} and three B^{I} nearest neighbors in its sub-cell. The different (111) planes are indicated.

between a B^{I} and a B^{II} layer, these have five B^{II} and three B^{I} nearest neighbors. For $B^{I}=Li^{+}$ and $B^{II}=W^{6+}$ ($A^{1.67+}(Li_{1/3}W_{2/3})O_3$), the formal charge, q, on the octahedral framework in the A^{I} and A^{II} sub-cells = $\{[(6\times6+2\times1)/8]-6\}=-1.25$, and $\{[(5\times6+3\times1)/8]-6\}=-1.875$, respectively. If the A sites were occupied by a combination of cations with an average total charge of +1.67, the excess formal charge per sub-cell (Δq) is +0.417, and −0.208 at the A^{I} and A^{II} positions. This imbalance in the formal charge is larger than the value in $A^{2+}(B^{2+}_{1/3}B^{5+}_{2/3})O_3$ perovskites, where $\Delta q=+0.25$ and −0.125. Analysis of the local charge imbalance in $Ba[Li_{1/3}(Nb_{1/2}W_{1/2})_{2/3}]O_3$ reveals a similar instability. Here a 1:1 mixture of Nb:W with a mean charge of 5.5^{+} yields a formal framework charge = −1.625 and −2.1875 in the A^{I} and A^{II} sub-cells, and resultant $\Delta q=0.375$ and −0.1875. While the imbalance is again greater than in the BZT family of systems, the random occupancy of B^{II} by Nb and W will give a distribution of environments with much higher local imbalances that would range from $\Delta q=+0.75$ to 0.0 at A^{I}, and +0.125 to −0.5 at A^{II} for environments with Nb:W = 0:6 and 6:0, respectively. These local instabilities have been invoked previously to explain the destabilization of 1:2 ordering in (Na^{+}/La^{3+}) A-site substituted $(Na_{1/2}La_{1/2})(Mg_{1/3}Ta_{2/3})O_3$ and $(Na_{1/2}La_{1/2})(Mg_{1/3}Nb_{2/3})O_3$ perovskites [23], and we believe they are also responsible for the loss of 1:2 order in the W-rich BLNW solid solutions.

We now turn to the formation of the 1:1 ordered phases in the $(1-x)Ba(Li_{1/4}Nb_{3/4})O_3-(x)Ba(Li_{2/5}W_{3/5})O_3$ system, which is confined to an extremely narrow region at $x\approx0.833(5/6)$. The stoichiometry of a 1:1 ordered $Ba(B^{I}_{1/2}B^{II}_{1/2})O_3$ form of the BLNW solid solutions could be represented by the general formula $Ba\{Li_{1/2+3x/10}Nb_{1/2-x/2}W_{x/5}\}_{1/2}(Nb_{1-x}W_x)_{1/2}O_3$ (i.e. $(1-x)Ba(Li_{1/2}Nb_{1/2})_{1/2}(Nb)_{1/2})O_3-(x)$ $Ba(Li_{4/5}W_{1/5})_{1/2}(W)_{1/2})O_3$). However, for solid solutions with $x\geqslant5/6$, maximum avoidance of Li and W on the B^{I} site can be achieved if the Nb/W cations readjust their distribution to maintain complete occupancy of the B^{II} site by W. At $x=5/6$ there is complete avoidance of Li and W on B^{I} and complete occupancy of W on B^{II}, and the two sites in the 1:1 phase, $Ba(Li_{3/4}Nb_{1/4})_{1/2}W_{1/2}O_3$, have the highest possible difference in charge ($\Delta q=4$) and size ($\Delta r=0.13$), and the lowest possible on-site charge/size mismatch. For higher x, B^{I} must contain some occupancy by W and the overbonding of anions with two W neighbors will compromise the stability; at lower x ($0\leqslant x\leqslant5/6$) the stability will be reduced by a lower site size/charge difference. The thin sliver of stability of 1:1 order observed at $x=0.833$ is in excellent agreement with the predictions of this crystal chemical model. There is no composition in the BLNW system that forms a completely random B-site arrangement, even in the two-phase regions; this is further evidence for the instability of W–O–W linkages that have a greater probability being formed in a solid solution with a completely disordered B-site distribution at any value of x.

As noted earlier, the rigid stoichiometry of the 1:2 ordered BZT family is well known and the substitution of very low levels of a foreign ion of a different size onto the B^{I} or B^{II} sites induce a transition to a non-stoichiometric (random site), 1:1 ordered structure. However, as described in detail elsewhere (Wu and Davies, in preparation), in each of these cases the substitution reduces the charge difference of the two sites in the competing 1:2 structure to a value below 3. The observation of non-stoichiometry in the BLNW phases would suggest that 1:2 order can only be sustained when the substituents increase the charge difference (Δq) above 3. $Ba(Li_{1/4}Nb_{3/4})O_3$ can be viewed as an end-member where the free energy of a metastable, non-stoichiometric, 1:2 ordered arrangement, $Ba\{(Li_{3/4}Nb_{1/4})^{2+}\}_{1/3}\{Nb^{5+}\}_{2/3}O_3$, can be lowered below that of the other competing phases by introducing substituents that increase the size and charge difference of the B^{I} and B^{II} sites. In the BLNW system, the stabilization is realized by compensating the replacement of Nb^{5+} by W^{6+} on the B^{II} site by increasing the Li content on the B^{I} position according to the equilibrium:

$$(3/4Li^{+}+1/4Nb^{5+})_{B(I)}+(2Nb^{5+})_{B(II)}=(Li^{+})_{B(I)}+(W^{6+}+Nb^{5+})_{B(II)}.$$

It may be possible to stabilize other metastable, non-stoichiometric end-members; for example, $A^{2+}(Li^{+}_{2/3}Zr^{4+}_{1/3})_{1/3}(Nb)_{2/3}O_3$ could be a possible host for the substitutional stabilization of 1:2 order. By analogy with the BLNW system, the introduction of W^{6+} on the Nb site when compensated by an increase in the concentration of Li on the B^{I} site would increase the site charge/size difference in solid solutions such as $A^{2+}(Li_{(2/3+x/3)}Zr_{(1/3-x/3)})_{1/3}(Nb_{(1-x)}W_x)_{2/3}O_3$. These new target materials are currently being examined.

5. Conclusions

Cubic perovskites were found to be stable for the majority ($0.238\leqslant x\leqslant0.833$) of the solid solutions in the $(1-x)Ba(Li_{1/4}Nb_{3/4})O_3$–$(x)Ba(Li_{2/5}W_{3/5})O_3$ system. For $0.238\leqslant x\leqslant0.385$ the compositions adopt a single-phase 1:2 B-site ordered structure ($P\bar{3}m1$, $a\approx\sqrt{2}a_c$, $c\approx\sqrt{3}a_c$). In contrast to all the known 1:2 $Ba(B^{I}_{1/3}B^{II}_{2/3})O_3$ perovskites, the ordered BLNW solid solutions do not include any composition with a 1:2 cation stoichiometry and the two sites in the structure exhibit extensive non-stoichiometry ($Ba[(Li_{3/4+y/2}Nb_{1/4-y/2})_{1/3}(Nb_{1-y}W_y)_{2/3}]O_3$, $y=0.21-0.35$, where $y=0.9x$). The model for the structure was supported by refinements of

the site occupancies using neutron diffraction, and the range of stability can be explained by considering the site size/charge differences, the imbalance in the anion bond valences induced by W–O–W linkages, and the local charge imbalance at the *A*-site positions for W-rich compositions. These new 1:2 ordered phases are the first examples of a 1:2 ordered structure with a significant range of homogeneity. A single-phase 1:1 ordered "double perovskite" phase was observed at $x = 0.833$; the absence of any significant range of stoichiometry for the 1:1 order can also be interpreted in terms of the site charge/size differences, the on-site mismatches, and the instability of W–O–W linkages. In the microwave region, the 1:2 ordered phases exhibit reasonable quality factors; however, they are significantly lower than their stoichiometric $Ba(Zn_{1/3}Ta_{2/3})O_3$ counterparts.

Acknowledgments

This work was supported by the National Science Foundation (Grant No. DMR 02-13489), and made use of the MRSEC shared experimental facilities supported by the National Science Foundation through Grant No. DMR 00-79909. The assistance of Dr. Igor Levin and Dr. Brian Toby at the NIST with the neutron diffraction experiment is greatly appreciated. We also acknowledge the support of the National Institute of Standards and Technology, US Department of Commerce, in providing the neutron research facilities used in this work.

References

[1] F. Galasso, J. Pyle, Inorg. Chem. 2 (1963) 483.
[2] P.K. Davies, J. Tong, T. Negas, J. Am. Ceram. Soc. 80 (7) (1997) 1727–1740.
[3] M.A. Akbas, P.K. Davies, J. Am. Ceram. Soc. 81 (3) (1998) 670–676.
[4] A.Y. Borisevich, P.K. Davies, J. Solid State Chem. 170 (2003) 198–201.
[5] P.K. Davies, A. Borisevich, M. Thirumal, J. Eur. Ceram. Soc. 23 (2003) 2461–2466.
[6] L. Chai, M.A. Akbas, P.K. Davies, J.B. Parise, Mater. Res. Bull. 32 (9) (1997) 1261–1269.
[7] M.A. Akbas, P.K. Davies, J. Am. Ceram. Soc. 81 (4) (1998) 1061–1064.
[8] L. Chai, P.K. Davies, J. Am. Ceram. Soc. 80 (12) (1997) 3193–3198.
[9] B. Jancar, P.K. Davies, D. Suvorov, M. Valant, in: P. Glavic, D. Brodnjak-Voncina (Eds.), Zbornik Referatov s Posvetovanja Slovenski Kemijski Dnevi, Part 2, Univerza v Mariboru, Fakulteta za Kemijo in Kemijsko Tehnologijo, Maribor, Slovenia, 2002, pp. 808–813.
[10] T. Negas, R.S. Roth, H.S. Parker, W.S. Brower, J. Solid State Chem. 8 (1973) 1–13.
[11] A.C. Larson, R.B. Von Dreele, General Structure Analysis System, Report LAUR 86-748, Los Alamos National Laboratory, NM, 1994.
[12] G. Blasse, A.F. Corsmit, J. Solid State Chem. 10 (1974) 39–45.
[13] Fuming Jiang, Seiji Kojima, Changlei Zhao, Chude Feng, J. Appl. Phys. 88 (6) (2000) 3608–3612.
[14] A. Dias, V.S.T. Ciminelli, F.M. Matinaga, R.L. Moreira, J. Eur. Ceram. Soc. 21 (2001) 2739–2744.
[15] Lai-Cheng Tien, Chen-Chia Chou, Dah-Shyang Tsai, J. Am. Ceram. Soc. 82 (8) (2000) 2074–2078.
[16] I.D. Brown, D. Altermatt, Acta Crystallogr. B 41 (1985) 244–247.
[17] M.W. Lufaso, P.M. Woodward, Acta Crystallogr. B 57 (2001) 725–738.
[18] H. Vincent, Ch. Perrier, Ph. I'Heritier, M. Labeyrie, Mater. Res. Bull. 28 (1993) 951–958.
[19] L.H. Brixner, Mater. Res. Bull. 9 (1974) 1041–1044.
[20] Y. Hikichi, S. Suzuki, J. Am. Ceram Soc. 70 (5) (1987) C99–C100.
[21] J.-H. Park, P.M. Woodward, Inter. J. Inorg. Mater. 2 (2000) 153–166.
[22] K.R. Poeppelmeier, A.J. Jacoboson, J.M. Longo, Mater. Res. Bull. 15 (1980) 339–345.
[23] L. DuPont, L. Chai, P.K. Davies, Proceedings Materials Research Society, Solid State Chem. Inorg. Mater. II 547 (1999) 93–98.